AJPMHS GLOBAL RESEARCH NETWORK

AMERICAN Journal of Pediatric Medicine and Health Sciences
Volume 2, Issue 3, 2024 ISSN (E): 2993-2149

Thermal Analysis of Fe2O3/g-C3N4 Composite

Urinova Shahnoza Musurmon qizi, Urinov Alisher Musirmon o'g'li
Tashkent Institute of Chemical Technology, Alfraganus University

Abstract: Composites of graphitic carbon nitride with various metal oxides are widely used as photocatalysts. They are used as photocatalysts due to ease of synthesis steps, low cost of precursors, and high photocatalytic properties. One such composite photocatalyst is Fe2O3/g-C3N4 doped with Fe2O3.

Keywords: photocatalyst, Fe2O3/g-C3N4, diffractogram. thermal analysis.

Today, obtaining modified photocatalysts based on γ-C3N4 with photocatalytic activity is one of the urgent tasks [1]. Several methods are used to improve the catalytic efficiency of γ-C3N4-based photocatalysts and to facilitate the separation of holes and photogenerated electrons. These include methods such as doping different elements [2], joining two semiconductors [3], acid treatment [4] and modification with conjugated polymers [5].

During the analysis of the literature, the photocatalytic activity of the Fe2O3/g-C3N4 composite in the visible light range is higher than that of the pure g-C3N4. The photocatalytic activity of composites in the visible light field depends on the amount of Fe2O3, and as its amount increases, the photocatalytic property decreases. It was determined that the photocatalytic activity has a maximum value when Fe2O3/g-C3N4 (0.1%) is present [6].

Synthesis of γ-C3N4/Fe2O3 composite. For this, γ-C3N4 was first brought to a powder state and mixed with FeCl3□6H2O solution. Then, the dry mixture, which was dried and reduced to a powder state, was calcined in a special autoclave at 500 ℃ for 30 minutes. The composite synthesis process is as follows:

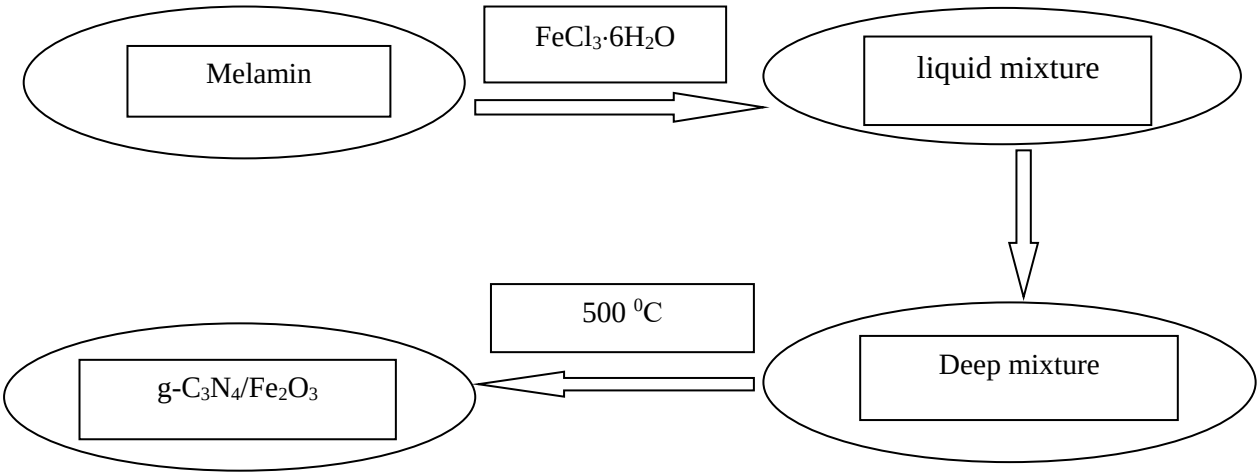

Fe (III) compounds are used as effective photocatalysts that improve the photocatalytic properties of semiconductor materials in the visible light range, and have the advantages of being cheap and occurring naturally in nature.

The synthesized O-g-C3N4/Fe2O3 new composite was identified by Fure-IR spectroscopy and compared with O-g-C3N4 Fure-IR spectroscopy of oxygen-doped graphitic carbon nitride. In our composite photocatalyst, a rather broad band was observed at 3152.17 and 3078.76 cm-1, which was caused by the collective symmetric and antisymmetric vibrations of –NH2, –NH, –OH, and 1623.92, 1533.27, 1453.33, 1312.47 peaks in cm-1 regions we can observe the vibrations of heterocyclic compounds belonging to CN. 887.20, 802.04, cm-1 corresponds to bending vibration of triazine ring, and vibrations in 590.07, 475.64 cm-1 correspond to Fe-O bonds. The IR spectrum of O-g-C3N4/Fe2O3 composite shows the presence of peaks corresponding to O-g-C3N4 and Fe2O3. The results of IR spectroscopy of the O-g-C3N4/Fe2O3 composite were confirmed by the results of X-ray phase analysis.

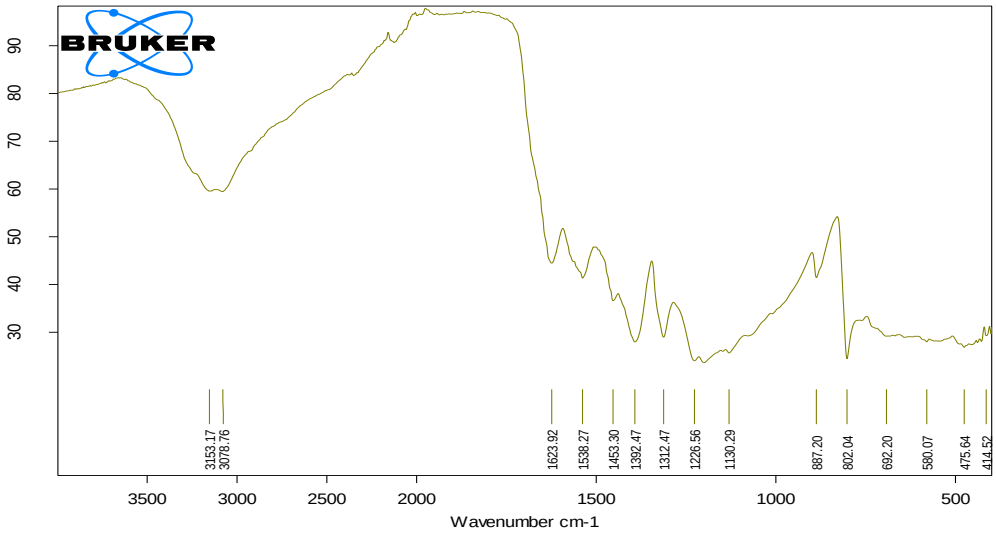

Figure 1. FURE IQ spectrum of O-g-C3N4/Fe2O3 photocatalyst

Analysis of Raman Spectroscopy Results of O-g-C3N4/Fe2O3 Photocatalyst.

The synthesized O-g-C3N4/Fe2O3 was identified using a new Raman spectroscopy method. In our composite photocatalyst, a rather broad band at 3000 and 3100 cm-1 was observed, which was caused by collective symmetric and antisymmetric vibrations – NH2 , – NH, –OH, and in the regions of 1628.69, 1484.54, 1310.40, 1232.21 cm-1 we can observe the vibrations of heterocyclic compounds belonging to peaks CN. 978.36, 767.01cm-1 corresponds to the bending vibration of the triazine ring, and vibrations in the 558.91, 475.77cm-1 region correspond to Fe-O bonds. The IR spectrum of O-g-C3N4/Fe2O3 composite shows the presence of peaks corresponding to O-g-C3N4 and Fe2O3. The results of O-g-C3N4/Fe2O3 composite were confirmed by Raman spectroscopy thermal analysis results.\

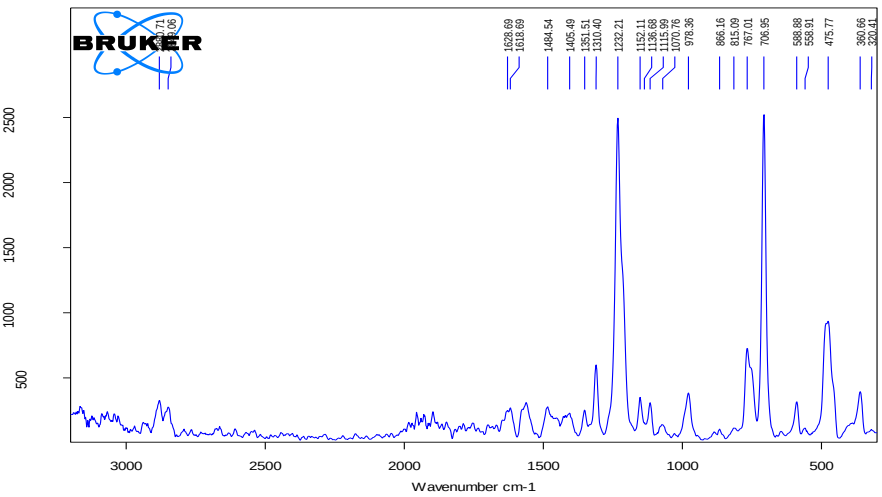

Figure 2. Raman spectrum of O-g-C3N4/Fe2O3 photocatalyst

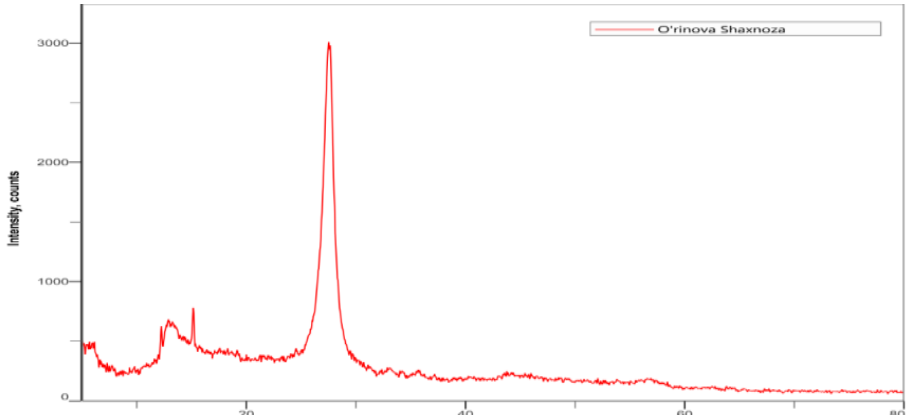

Figure 3. Diffractogram of O-g-C3N4/Fe2O3 photocatalyst.

It can be seen that in the X-ray analysis of O-g-C3N4/Fe2O3 composite photocatalyst, the two main peaks belonging to O-g-C3N4 are 2θ =27.17° and the lower shoulder peak is 2θ observed at =13.27°. The peaks related to Fe2O3 are not noticeable, because the intensity is low due to the very small amount of Fe2O3 in this composite. Crystallite sizes can be determined based on X-ray phase analysis data using Scherrer's formula.

№	2θ, °	d (Å)*	I/I1	B (FWHM)	D, нм
1.	13.21(4)	6.694(19)	222	3.37(13)	2.48
2.	15.18(3)	5.834(11)	222	0.16(3)	52.34
3.	27.552(17)	3.235(2)	1868	1.11(2)	7.70
4.	44.43(16)	2.037(7)	40	4.1(6)	2.19
5.	56.7(3)	1.621(8)	37	2.8(5)	3.37

From the data presented in Figure 3 and Table 1, it follows that the O-g-C3N4/Fe2O3 composite contains crystallites (particles) with a size of approximately 5 nm. Also, we can see that crystallites with a size of approximately 3 nm are present in significant intensity, and the proportion of crystallites with a size of approximately 3.37 nm is much lower according to the relative intensity of the peak (I/I1=37).

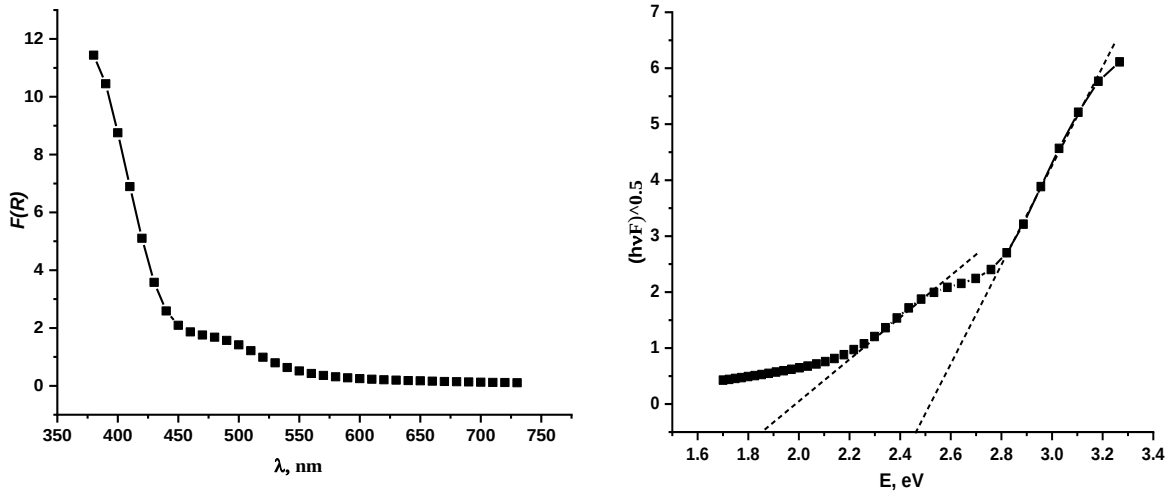

Figure 4. Light diffusion reflection spectrum (a) and Taus curve (b) of the synthesized O-g-C3N4-Fe2O3 photocatalyst

The bandgap width of the composite photocatalyst containing O-g-C3N4-Fe2O3 was determined graphically using the Taus curve (Fig. 4). In the Taus curve presented in Figure 4, there are 2 bending regions, which indicates that the composite has 2 forbidden region width (Eg) values,

respectively. The value of Eg in the high energy region (2.46 eV) corresponds to O-g-C3N4, the second value of Eg (1.85 eV) belongs to Fe2O3. It can be seen that the synthesized O-g-C3N4-Fe2O3 composite has a high potential for photocatalytic activity.

Analysis of thermal analysis results of O-g-C3N4/Fe2O3 photocatalyst.

The characteristics of the composition and structure of the obtained samples are also studied through the method of thermal analysis, which is widely used to determine the thermal stability of inorganic and organic substances, including graphite-like carbon nitride.

The derivatogram of the composite compound and the obtained results are presented in Figures 5-6.

In the results of thermal analysis, the nature of thermal effects, the observation of thermal decomposition of compounds, the temperature interval of effects and its nature, and the percentage mass loss in the same effect interval are presented. Thus, thermal analysis is widely used to study composite decomposition and liquefaction, phase changes, thermal decomposition, oxidation, combustion, intramolecular changes, and other processes. The study of the composition and structure of the synthesized composite was completed by obtaining their thermogravigrams.

The results of derivatography were analyzed in order to determine the thermal stability of the composite compound and the presence of water molecules in its composition. At the same time, it is determined that the mass of the sample, the mass of decomposition and the thermal stability of the complexes change with increasing temperature.

Thermal analyzes of the synthesized composite were performed in the temperature range from 20°C to 1000°C. Initially, 0.753 mg, i.e. 7.399% of the mass was lost in the range of 100-140 ^{o}C, this mass loss occurred due to the escape of water vapor and an exothermic effect was observed. Intensive mass loss in the range of 450-500 ^{o}C was 0.134 mg, i.e. 1.313%, and an exothermic effect was observed. In this case, the residual salts in the sample were oxidized. The final effects on the thermogravigrams of the composite synthesized at 560-800 ^{o}C are related to the formation of metal oxides. The amount of decay in this interval is 6.296% of decay, i.e. 0.641 mg. At a temperature of 747.17 ^{o}C, almost all the initial products decomposed, and the remaining metal oxide was observed to liquefy.

No change is observed after 800 ^{o}C . According to the results of the thermal analysis, it was found that the composition of the composite compound contains water molecules. As a result of thermolysis, metal oxide remains.

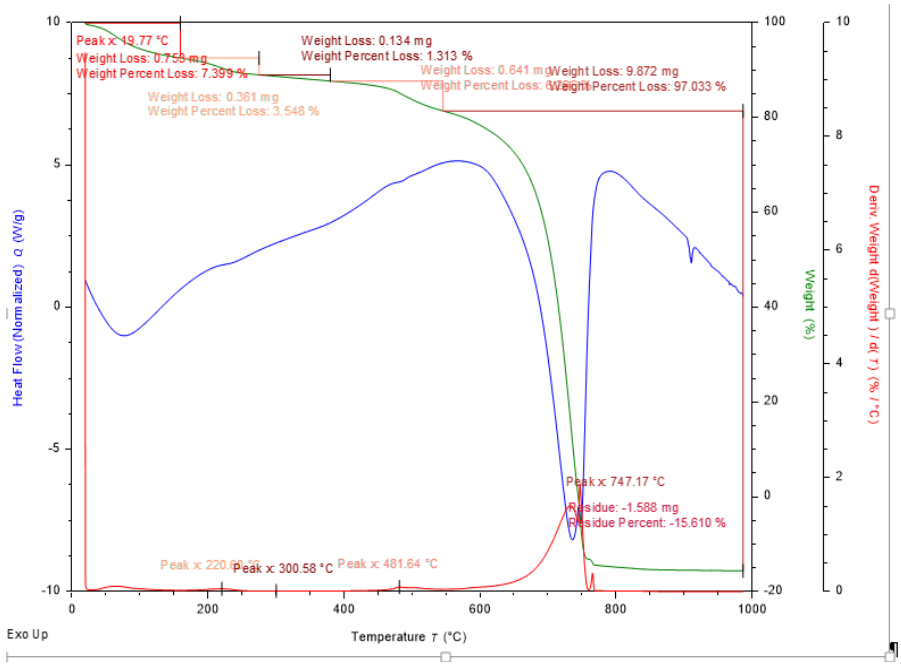

Figure 5. Thermal analysis graph of photocatalyst. Table 2.3

№	Time spent Δτ,min	Mass lost ,%	Temperature, °C	Amount of energy spent μV· s/mg
1	0,14	7,399	20	-1,68893
2	10,64	3,548	200	-0,05127
3	14,75	1,313	300	-0,01294
4	23,6	6,296	500	-0,08119
5	37,08	97,033	700	-1,88873

Figure 6. Thermal analysis results of photocatalyst.

Compound	Thermal effect Temperature	The nature of the thermo effect	Lost mass		Thermolysis product composition
			Found %	Estimated %	
O-g-C_3N_4/Fe_2O_3	20-140 ˚C	endo	97,033%	97,045%	–
	550-990 ˚C	endo			

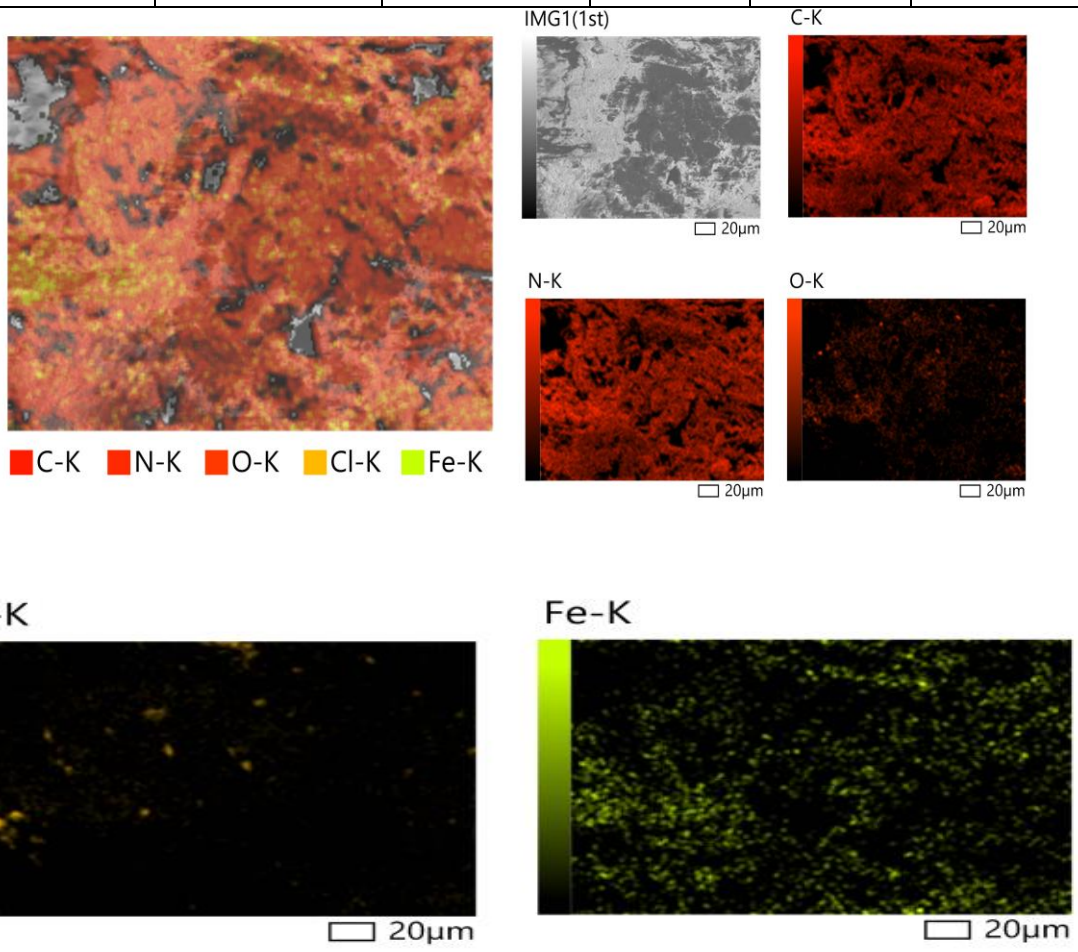

Bandwidth value made O-g-C3N4 nanolayer structure a promising material in environmental fields. The energy of the photon rays can exceed the bandwidth of the composite photocatalyst, and as a result, the electron in the valence region is excited to the conduction region (e-), leaving a gap (h+). This electron and the remaining valence field react with water or oxygen released from the reaction to form active oxygen and hydroxide, which in turn react and decompose organic pollutants in the system. Such photocatalytic dehydration has many advantages, including complete mineralization, low cost, and easy reaction conditions.

The decomposition of methylene blue in light was rapid and efficient in a short period of time. This is due to the formation of charge (hole/electron) carriers as a result of successive absorption of visible light photons on the surface of the photocatalyst. We use methylene blue (MB) as a standard pollutant to study the photocatalytic activity of the samples. For this, a 10 mg/l solution

of MB was prepared and 10 mg of catalyst was added. Experiments were conducted in sunlight. The samples were kept in a dark place for 1 hour in order for adsorption-desorption equilibrium to occur on the surface of the photocatalyst. Aliquots were taken every 10 minutes and concentration dependence of the catalyst was studied using a photoelectro colorimeter in the wavelength range of 390-680 nm. A magnetic transducer is used to perform this process and a photoelectrocolorimeter is used to determine the optical density. In the first step, the optical density of the standard solution of MB solution is checked. A nano catalyst is added to the MB solution and left for 20 minutes using a magnetic stirrer. Then, taking an aliquot part of the sample, the effect of the nanocatalyst on the concentration is checked. the same process is continued until the color of the solution (MB) changes, increasing the time by the same amount

$$g\text{-}C_3N_4/Fe_2O_3\ (h_{vq}^+) \rightarrow H_2O + {}^{\cdot}OH$$

$$g\text{-}C_3N_4/Fe_2O_3 + (e_{o'q}^-) \rightarrow O_2 \rightarrow O_{2\,ads}^{\cdot-}$$

$$O_2^{\cdot-} + H^+ \longrightarrow {}^{\cdot}OH_2$$

$$2e_{o'q} + H^+ + {}^{\cdot}OH_2 \longrightarrow {}^{\cdot}OH + OH^-$$

$$g\text{-}C_3N_4/Fe_2O_3(h_{vq}^+) + OH^- \rightarrow {}^{\cdot}OH$$

$$MK + {}^{\cdot}OH \longrightarrow \text{degradatsiya mahsuloti}$$

Photodegradation and mechanism of MK of 10 mg O-g-C3N4/Fe2O3 in sunlight visible field waves.

$$\eta = 1 - \frac{(C\tau - Co)}{Co}\ 100\%$$

η is the degradation rate, Cτ is the optical density of the solution at time t (Ct = At), Co is the initial optical density of the solution (Co = Ao)

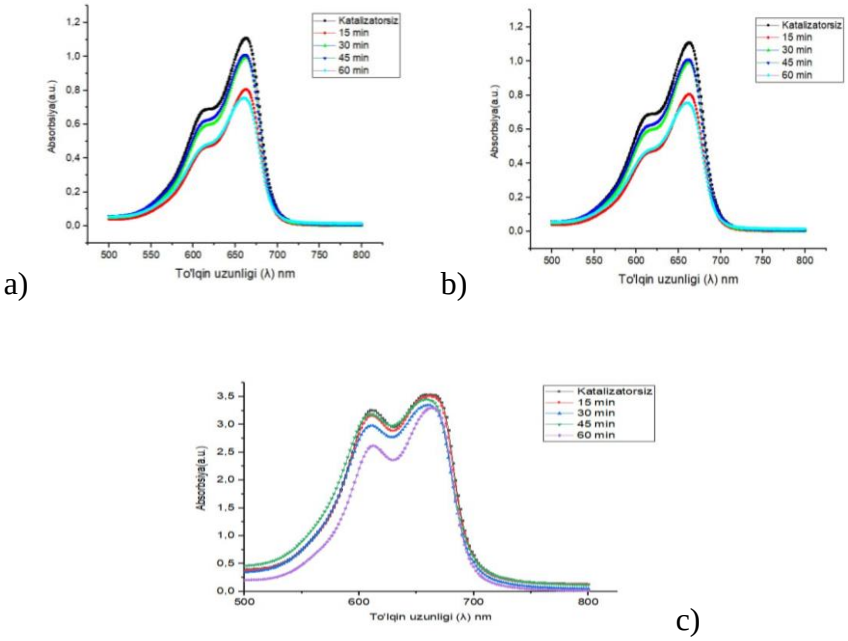

Figure 8. Photodegradation of O-g-C3N4/Fe2O3 composite 10 mg/ml (a), 20 mg/ml (b), 30 mg/ml (c) MK in sunlight visible field waves

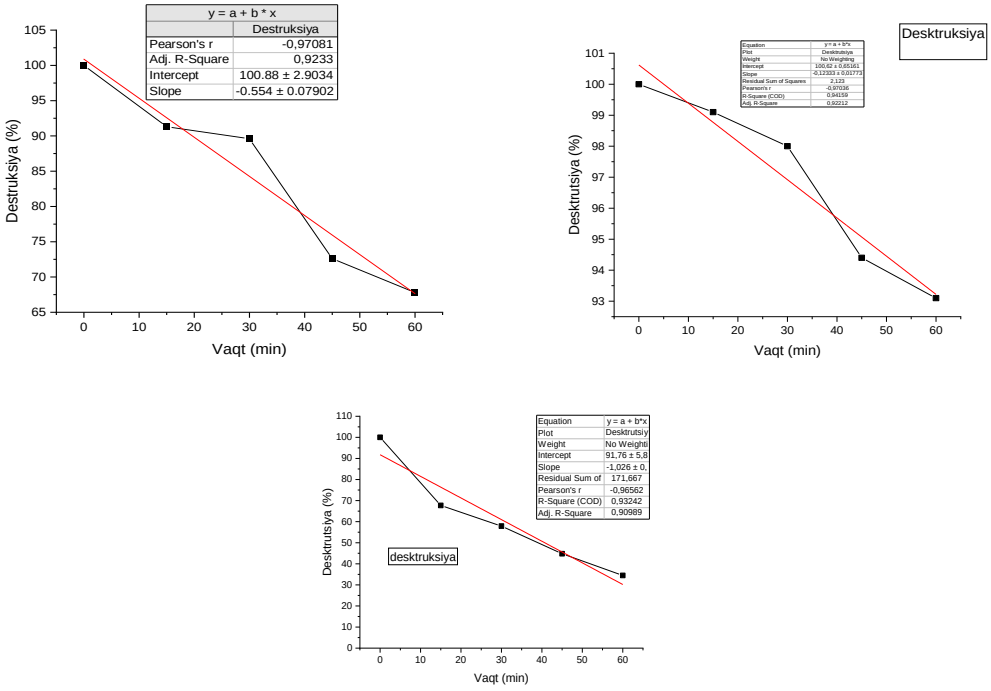

Figure 9. Kinetic modules of photodegradation rate of MK of O-g-C3N4/Fe2O3 compositions in sunlight visible field waves

The process of photodegradation was studied. A kinetic modular was used graphically to find the order of the reaction through time slices. The above graphs are satisfied for 1st order reactions and the correlation coefficients are somewhat close to 1.

The decomposition of methylene blue in light was rapid and efficient in a short period of time. This is due to the formation of charge (hole/electron) carriers as a result of successive absorption of visible light photons on the surface of the photocatalyst. As a result, more OH radicals are formed. O-g-C3N4 is a photocatalyst, and the addition of Fe2O3 to its composition has been studied to increase its performance. As a result, the optical band gap was 1.55 eV when studied. This result proves its photocatalytic activity. Scheme 2 depicts the photocatalytic process. The reactions that occur in this process are as follows:

Step 1 O-g-C3N4/Fe2O3 absorbs photons to form charge carriers

Step 2 Charge carrier diffusion

Stage 3 - formation of hydroxyl (.OH) and superoxide (O2-.) radicals

In conclusion, superoxide radicals formed react with the remaining particles in the system and form hydroxyl (OH) radicals. This causes methylene blue to oxidize and decompose. The photocatalysis process was also performed for pure O-g-C3N4. The comparison showed that the photocatalytic activity increased in the obtained composition. In the first 10 minutes, MB decomposition was 75% in pure O-g-C3N4, while this result reached 82% for the composite. This is evidence of a synergistic effect in the composition, and the particle absorbs the photon rays well in the first minutes. The degradation yield reached 94% within 60 minutes. The reaction order found graphically helps to make some assumptions about the process. If the 1st-order reaction is determined, it means that the reaction rate depends only on the concentration of 1 substance, and it means that a catalytic process has taken place in the system. So, only the concentration of MK in the system has decreased. The composition acted as a catalyst in the system

List of used literature:

1. B. Dianna, H. Uresti, A. Juan, A. Martinez. Photocatalytic degradation of RhB with microwave-prepared PbMoO4. J. Microw. Power Electromagn. Energy, 46(2012). p. 163
2. Hong, J., Xia, X., Wang, Y., Xu, R. Mesoporous carbon nitride with in situ sulfur doping for enhanced photocatalytic hydrogen evolution from water under visible light // J. Mater. Chem. 2012, 22, 15006–15012.
3. Ding, Z., Chen, X., Antonietti, M., Wang, X. Synthesis of Transition Metal-Modified Carbon Nitride Polymers for Selective Hydrocarbon Oxidation // ChemSusChem 2011, 274–281.
4. Yong-Jun Yuan,, Zhikai Shena, Shiting Wua, Yibing Sub, Lang Peia, Zhenguo Jia, Mingye Dinga, Wangfeng Baia, Yifan Chena, Zhen-Tao Yub, Zhigang Zoub, Liquid exfoliation of g-C3N4 nanosheets to construct 2D -2D MoS2/γ-C3N4 photocatalyst for enhanced photocatalytic H2 production activity, Applied Catalysis B: Environmental 246 (2019) 120–128.
5. A.B. Bogomolov, S.A. Kulakov, P.V. Zinin, V.A. Kutvitsky, M.F. Bulatov. Poluchenie fluorestsentnyx kompozitnyx materialov na osnove grafitopodobnogo nitrida carbona // Optika i spektroskopyia, 2020, tom 128, vyp. - S. 910-913.
6. Sidrasulieva G.B., Kattaev N.T., Akbarov X.I. Synthesis of nano-sized graphite carbon nitride g-O-C3Nx // Universum: chemistry and biology. - Moscow, 2021. - No. 12 (90). - S. 84-88.